Astronomy & Astrophysics manuscript no. master
February 6, 2017
©ESO 2017

High resolution near-IR spectroscopy of Arcturus and 10 Leo

Refining a near-IR iron line list

D. T. Andreasen[1,2], S. G. Sousa[1], E. Delgado Mena[1], N. C. Santos[1,2], and T. Lebzelter

[1] Instituto de Astrofísica e Ciências do Espaço, Universidade do Porto, CAUP, Rua das Estrelas, 4150-762 Porto, Portugal e-mail: daniel.andreasen@astro.up.pt
[2] Departamento de Física e Astronomia, Faculdade de Ciências, Universidade do Porto, Rua Campo Alegre, 4169-007 Porto, Portugal
[3] Departamento de Física, Universidade Federal do Rio Grande do Norte, 59072-970 Natal, RN, Brazil

Received ...; accepted ...

ABSTRACT

Context. Effective temperature, surface gravity, and metallicity are basic spectroscopic stellar parameters necessary to characterize a star or a planetary system. Reliable atmospheric parameters for FGK stars have been obtained mostly from methods that relay on high resolution and high signal-to-noise optical spectroscopy. The advent of a new generation of high resolution near-IR spectrographs opens the possibility of using classic spectroscopic methods with high resolution and high signal-to-noise in the NIR spectral window.
Aims. tralala
Methods. Our spectroscopic analysis is based on the iron excitation and ionization balance done in LTE. We use a high resolution and high signal-to-noise ratio spectrum of the Sun from the Kitt Peak telescope as a starting point to compile the iron line list. The oscillator strengths ($\log gf$) of the iron lines were calibrated for the Sun. The abundance analysis was done using the MOOG code after measuring equivalent widths of 357 solar iron lines.
Results. tralala

Key words. data reduction: high resolution spectra – stars individual: Arcturus – stars individual: 10 Leo

1. Introduction

Effective temperature ($T_{\rm eff}$), surface gravity ($\log g$), and metallicity ([M/H], where iron is normally used as a proxy) are fundamental atmospheric parameters necessary to characterise a single star, and to determine other indirect fundamental parameters such as mass, radius, and age from stellar evolutionary models (see e.g. Girardi et al. 2000; Dotter et al. 2008; Baraffe et al. 2015). Precise and accurate stellar parameters are also essential in exoplanet searches. Planetary radius and mass are mainly found from lightcurve analysis and radial velocity analysis, respectively. The determination of the mass of the planet implies a knowledge of the stellar mass, while the measurement of the radius of the planet is dependent on our capability to derive the radius of the star (see e.g. Torres et al. 2008; Ammler-von Eiff et al. 2009; Torres et al. 2012).

The derivation of precise stellar atmospheric parameters is not a simple task. Different approaches often lead to discrepant results (see e.g. Santos et al. 2013). Interferometry is usually considered an accurate method for deriving stellar radii (e.g. Boyajian et al. 2012); however, it is only applicable for bright nearby stars. Asteroseismology, on the other hand, reveals the inner stellar structure by observing the stellar pulsations at the surface. From asteroseismology it is possible to measure the surface gravity and mean density, and therefore to calculate the mass and radius (e.g. Kjeldsen & Bedding 1995).

A crucial parameter for the indirect determination of stellar bulk properties is the effective temperature. In that respect, the infrared flux method (IRFM) has proven to be reliable for FGK dwarf and subgiant stars. However, the IRFM needs a priori knowledge of the bolometric flux, reddening, surface gravity, and stellar metallicity (Blackwell & Shallis 1977; Ramírez & Meléndez 2005; Casagrande et al. 2010).

Finally, the use of high resolution spectroscopy along with stellar atmospheric models is an extensively tested method that allows the derivation of the fundamental parameters of a star (see e.g. Valenti & Fischer 2005; Santos et al. 2013). The procedure depends on the quality of the spectra, their resolution, and wavelength region. For low resolution spectra ($\lambda/\Delta\lambda < 20\,000$) the preferred method is to fit the overall observed spectrum with a synthetic one (see e.g. Recio-Blanco et al. 2006). Higher resolution spectra of slowly rotating stars (below 10 to 15 km/s) are in the regime where the equivalent width (EW) method can be used (see e.g. **?**, for details).

The derivation of stellar atmospheric parameters from high resolution spectra in the optical is now based on a standard procedure (see e.g. Valenti & Fischer 2005; Sousa et al. 2008). With the advancement of high resolution near-infrared (NIR) instruments, we will now be able to use a similar technique to that used in the optical part of the spectrum (see e.g. Meléndez & Barbuy 1999; Sousa et al. 2008; Tsantaki et al. 2013; Mucciarelli et al. 2013; Bensby et al. 2014). At the moment, the GIANO spectrograph installed at *Telescopio Nazionale Galileo* (TNG) is already available (Origlia et al. 2014), the *infrered doppler instrument* (IRD) installed at the Subaru telescope (Kotani et al. 2014), as is *Calar Alto high-Resolution search for M dwarfs with Exoearths with Near-infrared and optical Échelle Spectrographs* (CARMENES) for the 3.5 m telescope at Calar Alto Observatory (Quirrenbach et al. 2014). Two new spectrographs are planned for the near future: 1) The *CRyogenic InfraRed Echelle Spectro-*

graph Upgrade Project (CRIRES+) at the *Very Large Telescope* (VLT) (Follert et al. 2014) with expected first light in 2017, and 2) *un SpectroPolarimètre Infra-Rouge A Near-InfraRed Spectropolarimeter* (SPIRou) at *The Canada-France-Hawaii Telescope* (CFHT) (Delfosse et al. 2013; Artigau et al. 2014) with expected first light in 2017 as well. The spectral resolutions for these spectrographs range between 50 000 and 100 000.

With the advance of NIR spectrographs, we are yet to be to ready for the analysis of the data arriving at the moment and in the future. The analysis of stellar spectra is well understood for FGK stars in the optical part of the spectrum, however some work still needs to be done for the NIR part.

In this work we analyse the atlas of Arcturus (K0III) and the spectrum 10 Leo (K1III). The atlas of Arcturus was aquired at Kitt Peak National Observatory using the FTS spectrograph at the Mayall telescope (Hinkle et al. 2003) and 10 Leo from CRIRES (Nicholls et al. 2016). For the analysis we use the iron line list presented in Andreasen et al. (2016). This work serve as a continuation of our previous work.

The paper is organized as follows. In Sect. 2 we present the data we have aquired for this work along with some information of the two stars we will analyse. in Sect. 3 we refine the iron line list in order to get more reliable stellar parameters. The results are presented in Sect. 4 before we discuss our results in Sect. 6.

2. Data

While the community is currently on the verge to access of a large amount of high resolution NIR spectra with e.g. the spectrographs used here, the available spectra at the moment are sparse. We chose to use two stars cooler than the Sun since we showed in Andreasen et al. (2016) that this method works for a star hotter than the Sun (HD20010).

We have collected the atlas of Arcturus, one of the brightest stars on the Nothern hemisphere. Thus it is well studied (see e.g. Griffin & Griffin 1967; McWilliam 1990; Ramírez et al. 2013, to mention a few). We use the atlas from Hinkle et al. (2003) which covers the spectral range of interest (YJHK bands). Strong telluric features were identified with a spectrum from the TAPAS web page (Bertaux et al. 2014). The atlas also comes with the telluric from a telluric standard and the ratio of the two spectra in order to correct for the tellurics. We use both, but note that the telluric correction for Arcturus is not of the same quality as for 10 Leo as described below.

The second spectrum we have achieved is from the CRIRES-POP team (Nicholls et al. 2016). 10 Leo is a very similar star to Arcturus, which is also one reason this star was the first to be fully reduced by the team. It is a great help to be able to compare with the atlas of Arcturus. The main difference is the metallicity of the two stars, where Arcturus is metal poor and 10 Leo has solar metallicity. due to a telluric that could not be properly removed, low S/N, bad pixels, etc. Rather than giving an uncertain interpolation, Nicholls et al. (2016) decided to leave small gaps in the data. This have very little affect on this analysis. However, we were unable to measure one Fe II line, which are very important to determine the surface gravity.

A small summarise of the data is given in Tab. 1. The data is very similar, with similar S/N which is an approximately value measured with IRAF. The resolutions of the two spectrographs used are the same.

In Fig. 1 we compare the spectra of the two stars in a region with some of the iron lines used for the analysis described below.

3. Refining the NIR line list

Besides testing the line list at cooler effective temperatures with two K stars, we also want to refine the line list. This includes identifying recurring outliers, and lines which we are not able to measure, e.g. if a line is amidst a forrest of telluric lines. Hence, de-blending is nearly impossible. The first step was to go back and have a second look at the solar atlas used in Andreasen et al. (2016). We removed 342 Fe I lines and 13 Fe II lines in the process. Most of these were blended with other tellurics while a few were blended with other stellar absorption lines. We are down to 84 Fe I lines and 5 Fe II lines. The Fe II lines are used to determine $\log g$ by imposing ionization balance with Fe I. However, the low number of Fe II lines available is a concern, since the average abundance of Fe II is less trustworthy. One might fix $\log g$ during the process of obtaining stellar parameters, but this has an impact on the other derived parameters. It is better to leave $\log g$ free if possible, and either make corrections at the end or change it to a value from a more reliable source. This could for example be asteroseismology or from the parallaxes measured with Gaia.

4. Results

We derive the stellar atmospheric parameters in the same way as described in Andreasen et al. (2016) using FASMA (**?**). The EWs are measured for both stars automatically with ARES (Sousa et al. 2015) and by hand with splot in IRAF. We compare the derived stellar parameters from the two measured sets of EWs.

4.1. Arcturus

Arcturus is one of the brightest stars on the night sky with a V magnitude of -0.05 (Ducati 2002). Hence it is a prime target for testing the line list by Andreasen et al. (2016) with numerous measurements as mentioned above.

Lines blended with telluric were omitted from the analysis. The equivalent width (EW) of rest of the lines were measured by hand using the splot function in IRAF. In the atlas there exist both a summer observation set and a winter observation set. This is in order to minimize the effect of tellurics at different spectral regions. As many lines as possible were measured in both sets. The EW measurements from the different data sets and method (automatic and manual) can be seen in Fig. 2. Parameters were derived from the manual measurements and from the automatic (using both the summer and winter set). For all three sets parameters were derived with and without $\log g$ fixed. The derivation follows the procedure presented in Andreasen et al. (2016) with removal 1 outlier iteratively after the minimization routine (**?**) reach convergence. The final results are presented in Tab. 2.

We generally see good agreement between the derived parameters and the values from the literature. The only parameter being difficult to measure is the surface gravity due to the lack of Fe II lines in the NIR. The metallicity is very important to derive accurately, and we report good results overall, but especially with the automatic measurements, compared to literature values. For visualization the parameters are plotted (except $\xi_{\rm micro}$) in Fig. 3.

4.2. 10 Leo

The approach for determining the atmospheric stellar parameters for 10 Leo is identical as for Arcturus. The final reduced data is divided in YJ, H, and K bands. We use ARES on each band separately. For the small gaps in the spectrum, we simply set the

Table 1. The spectra and spectral type (from Simbad) of our sample with the corresponding spectrograph used to acquire the data and its spectra resolution. In the last column we show the S/N measured with splot in IRAF.

Star	Spectral type	Spectrograph	Resolution	S/N
Arcturus	K0III	FTS	100 000	300
10 Leo	K1III	CRIRES	100 000	300

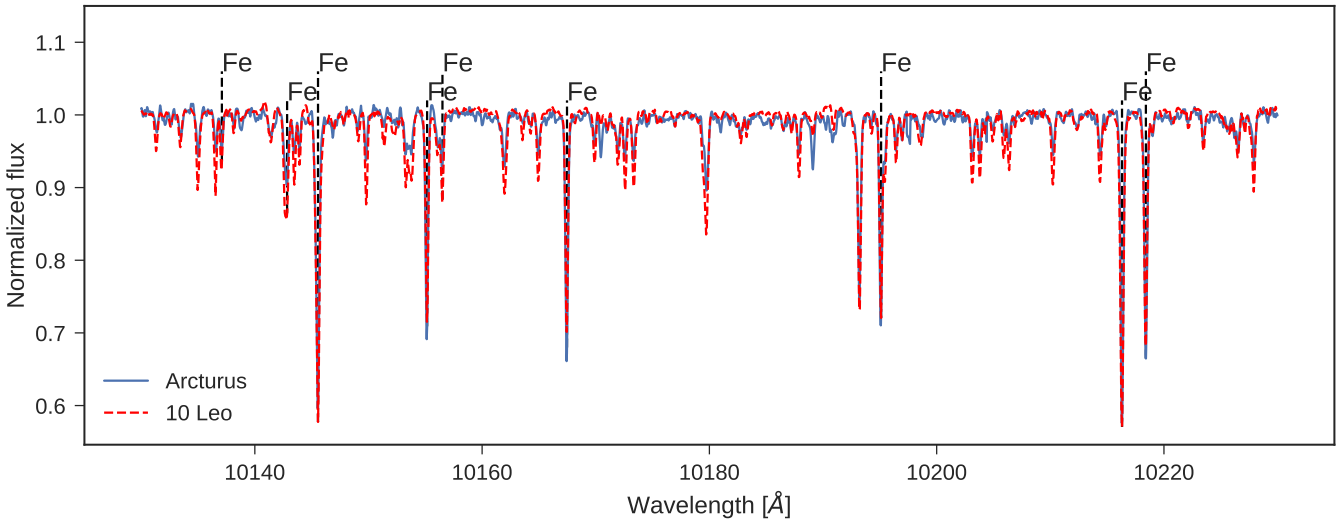

Fig. 1. The spectrum of the two stars, in blue is Arcturus, and green is 10 Leo. We mark the location of Fe I lines in the region.

Table 2. The derived parameters for Arcturus with and without fixed surface gravity after 3σ outlier removal. The litereature values are a simple mean of all the available parameters on Simbad with the corresponding standard error. There is no microturbulence available, so we derived it ourself using the empirical relation from Adibekyan et al. (2015) for each set of parameters.

	$T_{\rm eff}$ (K)	$\log g$ (dex)	$\xi_{\rm micro}$ (km/s)	[Fe/H] (dex)
Literature	4306 ± 100	1.69 ± 0.32	1.92 ± 0.15	−0.54 ± 0.11
IRAF	4380 ± 79	0.64 ± 0.33	1.14 ± 0.09	−0.49 ± 0.07
IRAF	4212 ± 77	1.69 (fixed)	1.25 ± 0.08	−0.37 ± 0.03
ARES (summer)	4439 ± 63	1.20 ± 0.20	1.55 ± 0.10	−0.58 ± 0.06
ARES (summer)	4348 ± 75	1.69 (fixed)	1.58 ± 0.09	−0.53 ± 0.03
ARES (winter)	4436 ± 67	0.55 ± 1.77	1.35 ± 0.09	−0.56 ± 0.07
ARES (winter)	4233 ± 109	1.69 (fixed)	1.43 ± 0.09	−0.49 ± 0.04
Weighted mean	4421 ± 40	0.96 ± 0.60	1.34 ± 0.05	−0.55 ± 0.04
Weighted mean	4269 ± 51	1.69 (fixed)	1.41 ± 0.05	−0.46 ± 0.02

value to 1, since the spectrum is already normalized. This will also prevent ARES to measure any lines in these regions. The EWs from the three regions are combined to one final line list used for the determination of the parameters. We list the result in Tab. 3 alongside with a mean of literature values taken from Simbad.

Generally the derived parameters are in excellent agreement with the literature values listed here. Surprisingly we are able to derive good $\log g$ values, although quite large errors and consistently lower, compared to the results from Arcturus.

A synthetic spectrum with the best parameters for both stars can be seen in Fig. 4. The region is the same as in Fig. 1.

5. Discussion

6. Conclusion

Being able to successfully determine parameters for two early K giants, we are now making the bridge for the line list towards cooler temperatures. The obvious next step is the even colder M stars. Particular interesting are the M dwarfs known to be prone forming rocky planets.

Acknowledgements. This work was supported by Fundação para a Ciência e a Tecnologia (FCT) through the research grants UID/FIS/04434/2013 and PTDC/FIS-AST/1526/2014. N.C.S., and S.G.S. acknowledge the support from FCT through Investigador FCT contracts of reference IF/00169/2012, and IF/00028/2014, respectively, and POPH/FSE (EC) by FEDER funding through the program "Programa Operacional de Factores de Competitividade - COMPETE". E.D.M. acknowledge the support from FCT in form of the fellowship SFRH/BPD/76606/2011. This work also benefit from the collaboration of a cooperation project FCT/CAPES - 2014/2015 (FCT Proc 4.4.1.00 CAPES). This research has made use of the SIMBAD database operated at CDS, Strasbourg (France). This work has made use of the VALD database, operated at Uppsala University, the Institute of Astronomy RAS in Moscow, and the University of Vienna.

References

Adibekyan, V. Z., Benamati, L., Santos, N. C., et al. 2015, MNRAS, 450, 1900

Table 3. Same as Tab. 2. The errors on $T_{\rm eff}$ and $\xi_{\rm micro}$ for the weighted mean with fixed $\log g$ are mathematically lower than reported, but we chose to set a lower limit. These errors are underestimated.

	$T_{\rm eff}$ (K)	$\log g$ (dex)	$\xi_{\rm micro}$ (km/s)	[Fe/H] (dex)
Literature	4720 ± 42	2.54 ± 0.11	1.59 ± 0.02	0.00 ± 0.03
IRAF	4835 ± 85	2.41 ± 0.41	1.28 ± 0.08	0.09 ± 0.06
IRAF	4768 ± 88	2.54 (fixed)	1.20 ± 0.08	0.01 ± 0.05
ARES	4805 ± 98	2.42 ± 0.61	1.23 ± 0.10	−0.01 ± 0.07
ARES	4768 ± 105	2.54 (fixed)	1.20 ± 0.10	−0.01 ± 0.06
Weighted mean	4821 ± 65	2.41 ± 0.37	1.26 ± 0.06	0.04 ± 0.05
Weighted mean	4768 ± 69	2.54 (fixed)	1.20 ± 0.06	0.05 ± 0.04

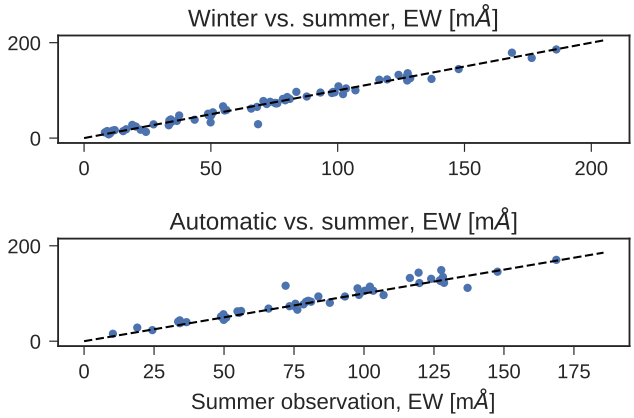

Fig. 2. Top figure: compare the manuel EWs measurement between the summer observations and winter observations. Bottom figure: Same as above, but with automatic measurements from ARES (summer) and manuel measurements (summer).

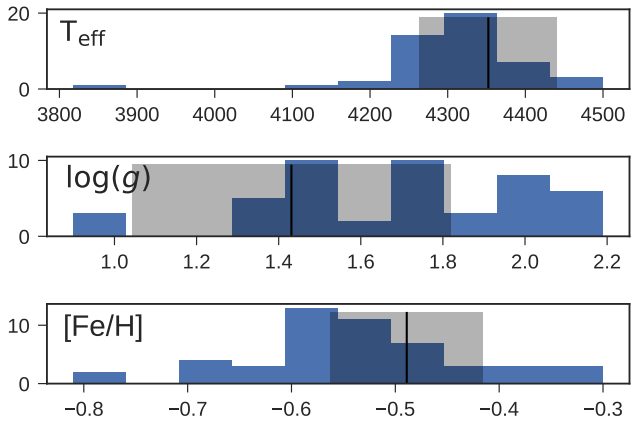

Fig. 3. Histogram of the atmospheric stellar parameters of Arcturus (except $\xi_{\rm micro}$). The black vertical lines are the derived parameters, and the gray shaded area are the errors on the corresponding parameters.

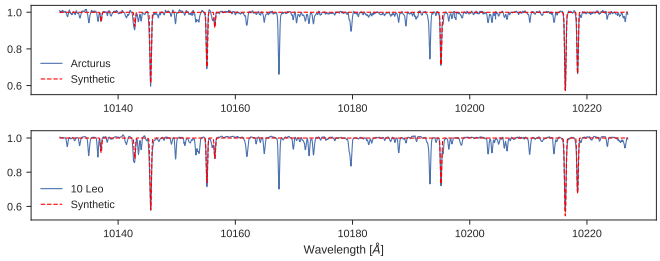

Fig. 4. Synthetic fit of both stars with the parameters from the weighted mean.

Ammler-von Eiff, M., Santos, N. C., Sousa, S. G., et al. 2009, A&A, 507, 523
Andreasen, D. T., Sousa, S. G., Delgado Mena, E., et al. 2016, A&A, 585, A143
Artigau, É., Kouach, D., Donati, J.-F., et al. 2014, in Society of Photo-Optical Instrumentation Engineers (SPIE) Conference Series, Vol. 9147, Society of Photo-Optical Instrumentation Engineers (SPIE) Conference Series, 15
Baraffe, I., Homeier, D., Allard, F., & Chabrier, G. 2015, A&A, 577, A42
Bensby, T., Feltzing, S., & Oey, M. S. 2014, A&A, 562, A71
Bertaux, J. L., Lallement, R., Ferron, S., Boonne, C., & Bodichon, R. 2014, A&A, 564, A46
Blackwell, D. E. & Shallis, M. J. 1977, MNRAS, 180, 177
Boyajian, T. S., von Braun, K., van Belle, G., et al. 2012, ApJ, 757, 112
Casagrande, L., Ramírez, I., Meléndez, J., Bessell, M., & Asplund, M. 2010, A&A, 512, A54
Delfosse, X., Donati, J.-F., Kouach, D., et al. 2013, in SF2A-2013: Proceedings of the Annual meeting of the French Society of Astronomy and Astrophysics, ed. L. Cambresy, F. Martins, E. Nuss, & A. Palacios, 497–508
Dotter, A., Chaboyer, B., Jevremović, D., et al. 2008, ApJS, 178, 89
Ducati, J. R. 2002, VizieR Online Data Catalog, 2237
Follert, R., Dorn, R. J., Oliva, E., et al. 2014, in Society of Photo-Optical Instrumentation Engineers (SPIE) Conference Series, Vol. 9147, Society of Photo-Optical Instrumentation Engineers (SPIE) Conference Series, 19
Girardi, L., Bressan, A., Bertelli, G., & Chiosi, C. 2000, A&A Supp., 141, 371
Griffin, R. & Griffin, R. 1967, MNRAS, 137, 253
Hinkle, K., Wallace, L., Livingston, W., et al. 2003, in Cambridge Workshop on Cool Stars, Stellar Systems, and the Sun, Vol. 12, The Future of Cool-Star Astrophysics: 12th Cambridge Workshop on Cool Stars, Stellar Systems, and the Sun, ed. A. Brown, G. M. Harper, & T. R. Ayres, 851–856
Kjeldsen, H. & Bedding, T. R. 1995, A&A, 293, 87
Kotani, T., Tamura, M., Suto, H., et al. 2014, in Society of Photo-Optical Instrumentation Engineers (SPIE) Conference Series, Vol. 9147, Society of Photo-Optical Instrumentation Engineers (SPIE) Conference Series, 14
McWilliam, A. 1990, ApJS, 74, 1075
Meléndez, J. & Barbuy, B. 1999, ApJS, 124, 527
Mucciarelli, A., Pancino, E., Lovisi, L., Ferraro, F. R., & Lapenna, E. 2013, ApJ, 766, 78
Nicholls, C. P., Lebzelter, T., Smette, A., et al. 2016, ArXiv e-prints [e-prints[arXiv]1609.07873]
Origlia, L., Oliva, E., Baffa, C., et al. 2014, in Society of Photo-Optical Instrumentation Engineers (SPIE) Conference Series, Vol. 9147, Society of Photo-Optical Instrumentation Engineers (SPIE) Conference Series, 1
Quirrenbach, A., Amado, P. J., Caballero, J. A., et al. 2014, in Society of Photo-Optical Instrumentation Engineers (SPIE) Conference Series, Vol. 9147, Society of Photo-Optical Instrumentation Engineers (SPIE) Conference Series, 1
Ramírez, I., Allende Prieto, C., & Lambert, D. L. 2013, ApJ, 764, 78
Ramírez, I. & Meléndez, J. 2005, ApJ, 626, 446
Recio-Blanco, A., Bijaoui, A., & de Laverny, P. 2006, MNRAS, 370, 141
Santos, N. C., Sousa, S. G., Mortier, A., et al. 2013, A&A, 556, A150
Sousa, S. G., Santos, N. C., Adibekyan, V., Delgado-Mena, E., & Israelian, G. 2015, A&A, 577, A67
Sousa, S. G., Santos, N. C., Mayor, M., et al. 2008, A&A, 487, 373
Torres, G., Fischer, D. A., Sozzetti, A., et al. 2012, ApJ, 757, 161
Torres, G., Winn, J. N., & Holman, M. J. 2008, ApJ, 677, 1324
Tsantaki, M., Sousa, S. G., Adibekyan, V. Z., et al. 2013, A&A, 555, A150
Valenti, J. A. & Fischer, D. A. 2005, ApJS, 159, 141